



Tatti, E., Duff, A., Kostrysia, A., Cholet, F., Ijaz, U. and Smith, C. (2022) Potential nitrification activity reflects ammonia oxidising bacteria but not archaea activity across a soil-sediment gradient. *Estuarine, Coastal and Shelf Science*, 264, 107666.

(doi: [10.1016/j.ecss.2021.107666](https://doi.org/10.1016/j.ecss.2021.107666))

This is the Author Accepted Manuscript.

There may be differences between this version and the published version. You are advised to consult the publisher's version if you wish to cite from it.

<https://eprints.gla.ac.uk/259377/>

Deposited on: 24 November 2021

Enlighten – Research publications by members of the University of Glasgow
<http://eprints.gla.ac.uk>

1 **Potential Nitrification Activity Reflects Ammonia Oxidising Bacteria but not Archaea**
2 **activity across a Soil-Sediment Gradient**

3 **Enrico Tatti¹, Aoife M Duff¹⁺, Anastasiia Kostrytsia², Fabien Cholet², Umer Z Ijaz², Cindy**
4 **J Smith^{1,2*}**

5 ¹Microbiology, School of Natural Sciences, National University of Ireland Galway, Galway,
6 Republic of Ireland

7 ²Infrastructure and Environment Research Division, James Watt School of Engineering,
8 University of Glasgow, Glasgow, UK

9 ***Correspondence:**

10 Cindy J Smith

11 cindy.smith@glasgow.ac.uk

12 ⁺current address: Teagasc, Johnstown Castle, Co Wexford, Y35 Y521

13 **Keywords:** nitrification; soil; sediments; Potential Nitrification Activity (PNA); *amoA*
14 transcripts; Republic of Ireland, Rusheen and Clew bays

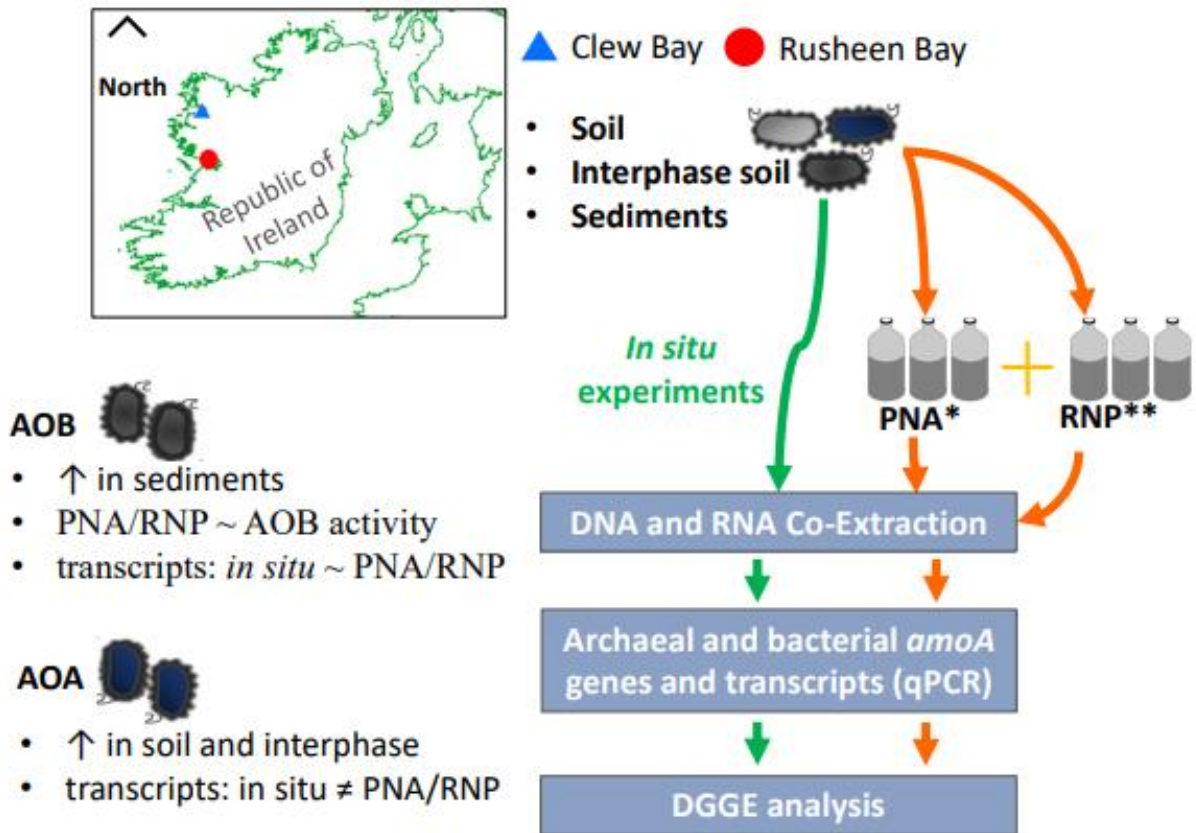
15 **Abstract**

16 Terrestrial-marine ecosystems have important ecologically relevant roles influencing the retention
17 and mobility of nitrogen entering coastal ecosystems. The sharp physico-chemical gradients
18 represent an ideal environment to elucidate the relative contributions of ammonia oxidizing
19 archaea (AOA) and bacteria (AOB) to the nitrification process. Here we examined the activity of
20 ammonia oxidisers (AO) across two coastal bays soil-sediment gradients to explore the functional
21 shift from AOA to AOB, and determine if transcriptional activity within the environment (*in situ*)

22 was emulated in laboratory potential nitrification activity incubations. To do this gene and
23 transcripts abundance and diversity were measured along with potential nitrification activity
24 (PNA) and recovery nitrification potential (RNP) from a series of soil, interface and sediment sites.
25 We compared the composition of *amoA* transcript community structure *in situ* vs. PNA/RNP to
26 see if the active AOA and AOB were similar in the environment and in the laboratory experiments.
27 AOA was dominant at gene and transcript level in soil and interphase sites, but active transcripts
28 *in situ* did not match those within the PNA/RNP assays. AOB was dominant at gene and transcript
29 level in sediments and here transcripts *in situ* and within the PNA/RNP were similar. A high
30 correlation between AOB transcripts and PNA in sediments was observed but a negative
31 correlation for AOA in soils was seen. Our data indicates that while the PNA/RNP may be a good
32 proxy for AOB activity in these sediments, it was not for AOA dominated soil due to unfavorable
33 incubation conditions.

34 Graphical Abstract

35



36

37 **Introduction**

38 Nitrogen (N) is an essential component of all living organisms and a significant controller of
39 primary production in marine and terrestrial environments. The N cycle is a complex combination
40 of assimilatory and dissimilatory biogeochemical pathways driven mainly by microorganisms
41 (Stein and Klotz, 2016). Nitrification plays a central role, oxidising ammonia to nitrite and nitrate
42 making nitrate/nitrite available for reduction and removal from the ecosystem by denitrification.
43 Nitrification is also directly linked to the carbon (C) cycle via autotrophic fixation of CO₂ (Gruber
44 and Galloway, 2008). Furthermore, it has been shown to be capable of generating notable amounts
45 of the noxious greenhouse gas N₂O via incomplete oxidation of hydroxylamine and/or nitrifier
46 denitrification (Yang et al., 2017).

47 Nitrification has long been defined as an aerobic two-step reaction carried out by both ammonia
48 oxidisers (AO), who convert ammonia (NH₄⁺) to nitrite (NO₂⁻), and nitrite oxidizing bacteria
49 (NOB), who convert NO₂⁻ to nitrate (NO₃⁻). AO includes both ammonia oxidizing bacteria (β- and
50 γ-proteobacteria; AOB) and ammonia oxidizing archaea (*Thaumarchaea*; AOA). Recently, the
51 classical view of nitrification, conducted by separate AO and NOB has been challenged by the
52 discovery of bacteria capable of complete oxidation of ammonium to nitrate (COMAMMOX).
53 Researchers have recently provided evidence that *Nitrospira spp.*, a genus previously considered
54 involved only in nitrite oxidation, is capable of complete oxidation of NH₄⁺ to NO₃⁻ (Daims et al.,
55 2015; van Kessel et al. 2015).

56 Ammonia oxidation has received significant attention in the literature and numerous studies have
57 been conducted to investigate the contribution of AOA and AOB to nitrification across different
58 natural and engineered ecosystems (e.g. Duff et al 2017; Fernandes et al., 2016; Gubry-Rangin et

59 al., 2010; Jäntti et al., 2018; Liu et al., 2013; Muukhtar et al., 2019; Yi et al., 2020; Zhang et al
60 2018;). A general understanding of the distribution and dominance of AOA and AOB has emerged
61 with AOB dominant in ammonia-rich coastal areas and estuaries (Duff et al., 2017; Lisa et al.,
62 2015; Mosier and Francis, 2008), wastewater (Bai et al., 2012) and N-rich grassland soils (Di et
63 al., 2009). AOA are more abundant in low-ammonium environments, such as ocean waters, river
64 sediment, freshwater lakes, and rice paddy soils (Li et al., 2015; Liu et al., 2013; Santos et al.,
65 2018) with pH as a further driver of niche differentiation in soils (Gubry-Rangin et al., 2010).
66 However, more recently AOAs with similar Km to *Nitrosomonas* have been isolated from soil
67 (Kits et al 2017; Hink et al., 2017). This, taken together with reports of AOA dominance in high-
68 ammonia estuaries (Moin et al., 2009; Cao et al., 2011), indicates that ammonia concentration
69 alone does not explain AO dominance and other factors such as pH (Gubry-Rangin et al., 2010)
70 and/or the source of ammonia nitrogen (organic vs. inorganic) may also play a role (Aigle et al.,
71 2020; Di et al., 2010).

72 In general, the relative contribution of AOB and AOA in the environment is determined by
73 quantification of *amoA* genes at DNA level, while nitrifier activity can be determined using ¹⁵N
74 isotopic approaches to measure *in situ* rates (Rysgaard et al., 1993; Hart et al., 1996). ¹⁵N
75 experiments tend to be time consuming and require access to specialized isotope ratio mass
76 spectrometry facilities. Alternatively, potential nitrification activity (PNA), is a simple, cheap and
77 fast approach that has been widely used in soil science (for a critical review see Hazard et al.,
78 2021) and to a lesser extent in coastal sediments (Li et al., 2014; Duff et al., 2017, Zhang et al.,
79 2019). PNA is not an *in situ* rate measurement, but a measure of the maximum capacity of a soil
80 or sediments nitrifying community to oxidise ammonia to nitrate under a given set of laboratory
81 conditions. Recovery of nitrification potential (RNP) is an extension of PNA (Taylor et al., 2010).

82 In RNP acetylene (C_2H_2) irreversibly stops the synthesis of the ammonia monooxygenase (AMO)
83 enzyme (Hyman and Wood, 1985), but upon removal, ammonia oxidation can resume the
84 synthesis of new AMO enzyme via transcription and translation.

85 However, there are some limitations to both *amoA* gene quantification and PNA. First, gene
86 abundance does not imply activity. Second, theoretically PNA/RNP reflects the maximum
87 nitrification/recovery rate of the community to an amendment of ammonia, it does not inform of
88 the individual contribution of AOB and AOA, nor if the organisms responding to the assay reflect
89 the *in situ* active organisms. Moreover, PNA is likely a biased measurement (Santoro et al., 2010)
90 which favors AOB due to the ammonia concentration supplied (100 μ M to 1 mM) (Duff et al.,
91 2017; Liu et al., 2013; Walkup et al., 2020). From enrichment cultures, it has been shown that the
92 growth rate of AOB is significantly reduced at NH_4^+ concentration between 39 μ M and 50 mM
93 (Koper et al., 2010; Park et al., 2009), while AOAs growth rate is lower at NH_4^+ concentrations
94 between 2 μ M and 2 mM (Koper et al., 2010). Therefore, PNA incubations do not inform what
95 organisms are responding to the assay, if these reflect the active AOs in the environment, and if
96 PNA is better suited to reflect AOB than AOA activity.

97 In this study, we explore the response of AOA and AOB to PNA and RNP across the terrestrial-
98 marine environment where we have previously shown the differing contribution of AOA and AOB
99 (Zhang et al., 2018). This work indicated that AOA were driving ammonia oxidation in soil and
100 AOB in sediments. This gradient provides an ideal site to disentangle the relationship between
101 gene and transcript abundance and PNA/RNP for AOB and AOA, respectively. We aimed to
102 understand the extent to which *amoA* gene and transcript abundance reflected PNA/RNP as a proxy
103 for AOB and AOA activity. We confirm the contribution of AOA and AOB across the soil and
104 sediment gradients via a series of PNA and RNP incubations with selective inhibitors combined

105 with quantification of the respective AOA and AOB *amoA* transcripts. Then using this gradient,
106 we explored the contribution of AOA and AOB to PNA and RNP, hypothesising that PNA activity
107 better reflects *in situ* active AOB than AOA.

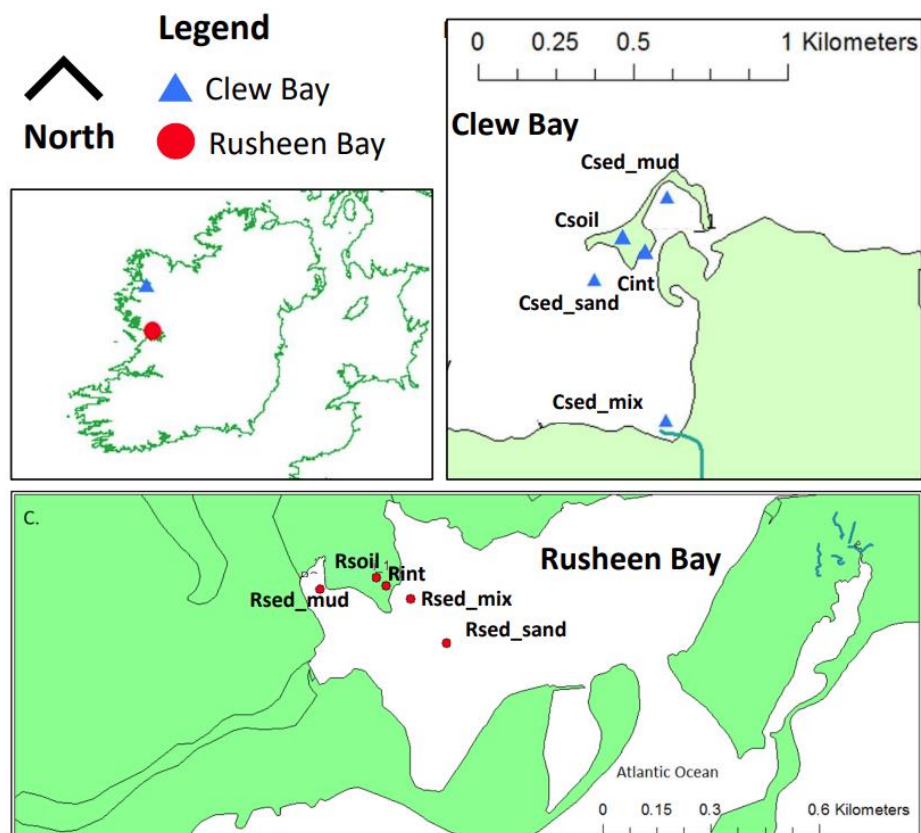
108

109 **Materials and Methods**

110 **Sites Descriptions and Sampling**

111 The study was carried out in two small (~ 1 km²) intertidal coastal bays - Rusheen and Clew bay
112 located on the west coast of the Republic of Ireland (**Fig. 1**). Rusheen bay (53° 25.5894'N, -9°
113 11.9532'W) is sheltered by a beach and is an intertidal mud/sand flat, situated along the north side
114 of Galway bay on the edge of Galway city (population 75000). Clew bay (53° 78.6962'N, -9°
115 64.9515'W) is an intertidal mud/sand flat situated in a rural area surrounded by agricultural land,
116 mainly sheep farming, approximately 120 km north-west of Rusheen Bay. A beach shelters the
117 bay on its seaward side. Numerous groundwater upwelling and freshwater streams are present in
118 the bay. Soil and sediment samples were collected in February 2015. In both bays, samples were
119 collected from five different points along a soil-benthic gradient based on previously performed
120 granulometric analysis (Duff et al., 2017; Zhang et al., 2018) (**Fig. 1**). The gradient originated near
121 the sea (i.e., 30 m) in vegetated soil (Rsoil and Csoil). It continued towards the water edge, into a
122 grass-covered interface zone where high tides occasionally submerge the soil with seawater (Rint
123 and Cint). Interface soils were water-logged and displayed signs of coastal erosion. The gradient
124 ended in coastal sediments of the intertidal zone characterized by different sand:mud ratio with
125 sediments characterized by a) high composition of mud (Rsed_mud and Csed_mud), b) a mix of

126 mud and sand (Rsed_mix and Csed_mix), c) sand only (Rsed_sand and Csed_sand) (Duff et al.,
127 2017; Zhang et al., 2018).



128
129 **Figure 1.** (A) Sampling locations are on the west coast of Ireland. Maps of Clew (B) and Rusheen
130 bays (C) depict the location of sampling sites along the soil-sediment gradients.

131 Soil and intertidal sediments (top 0-5 cm) were collected at low tide on February 23rd and 27th
132 2015 from Rusheen and Clew bay, respectively. Samples from ten random points within a 10 m²
133 area were pooled as one replicate with three such replicates collected from each 10 m² sample
134 location (**Fig. 1**). Replicates were homogenized, subsampled into 0.5 g aliquots, flash frozen and
135 then stored at -80°C for subsequent molecular analysis. These samples are referred to as the *in situ*
136 samples. Soil and sediment samples for PNA/RNP and physicochemical analysis were returned to

137 the lab on ice and stored at 4°C until analysis (performed not later than 6h from sampling). Soil
138 was manually broken up, removing stones and roots, and homogenized prior to PNA/RNP and
139 physico-chemical analysis.

140 **Determination of Physico-chemical Parameters**

141 Soil and sediment temperature was measured at each site with a mercury thermometer. Salinity of
142 site seawater was determined with a refractometer (Coral Farm, Ireland) and reported using with
143 the Practical Salinity Scale. Soil salinity was measured following extraction of pore-water after
144 centrifugation. pH was determined by mixing soil and sediments with deionised water at a ratio of
145 1:2 and measured with an Orion pH meter, model 420A (Cole Parmer, Ireland). Water content was
146 calculated via the weight loss of a known amount of sample dried at 105°C until a constant value
147 was reached (e.g., typically 24 h). Ammonium (NH₄⁺), nitrite (NO₂⁻) and nitrate (NO₃⁻) were
148 extracted from the sediment by incubating 5 g fresh weight (FW) sediment with 30 ml of 1 M KCl
149 for 1 h at 15°C on a shaker. Samples were then filtered with grade 52 Whatmann filter paper
150 (Fisher scientific, Ireland) and frozen at -20°C until further analysis. Dissolved inorganic nitrogen
151 (i.e., NO₂⁻, NO₂⁻+NO₃⁻ and NH₄⁺) was measured using colorimetric methods on a plate reader as
152 described by Bollmann et al. (2011). Dissolved organic carbon and nitrogen (DOC/DON) were
153 analysed from acidified samples on a Shimadzu TOC-L with TNM-L module. Limits of detection
154 are provided in supplementary information (Tab. S2).

155 **PNA, RNP and use of Selective Inhibitors**

156 PNAs were carried out in triplicate at all sites in both bays (**Fig. 1**). A schematic of the PNA and
157 RNP experiments can be found in **Tab. S1**. Five g of fresh weight (FW) soil or sediment was added
158 to 250 ml glass bottle (Voight, Kansas, USA) containing 30 ml of either phosphate-buffered saline

159 (PBS) 0.1 M pH 7.1 for soil and interface samples, (salinity adjusted to *in situ* values) or 0.2 μm -
160 filtered site water for sediments. All were amended with 24 μM sodium azide, an inhibitor of nitrite
161 oxidation (NaN_3 , nitrite oxidation inhibitor; Sigma, Ireland; Ginestet et al., 1998) and 250 μM
162 NH_4^+ [$(\text{NH}_4)_2\text{SO}_4$, Sigma, Ireland]. These conditions, in the absence of selective AO inhibitors,
163 were considered the standard PNA. Two additional PNA assays were set up to investigate the
164 contribution of ammonia oxidizing bacteria and archaea: a) PNA amended with 50 mM of
165 allylthiourea (ATU, Sigma, Ireland), as a selective inhibitor of the bacterial ammonia
166 monooxygenase, sequestering the Cu^{2+} ions (Wang et al., 2017); b) PNA amended with 75 μM of
167 cycloheximide (CHX, Sigma, Ireland), a eukaryote and archaeal inhibitor of protein synthesis
168 (Vajrjala et al., 2014; Wright et al., 2020). However, there are notable limitations to each inhibitor,
169 with some AOA sensitive to ATU (Lehtovirta-Morley et al., 2013; Shen et al., 2013) and some
170 AOA insensitive to CHX (Taylor et al, 2010). Therefore, we refer to ATU-sensitive and CHX-
171 sensitive ammonia oxidisers, as illustrated in **Fig. S1**. Soil and sediment slurries were incubated in
172 open bottles in the dark on a shaker at 90 rpm at 15°C for 48 h. Preliminary experiments showed
173 that these conditions were optimal for the measured rates, with aeration preventing N
174 immobilization and denitrification (data not shown). Background concentrations of NO_2^- were
175 measured after 10 mins of incubation. At the end of the experiments, NO_2^- was extracted with two
176 volumes of 1 M KCl following 30 min agitation at 90 rpm. Nitrite was measured as described
177 above. At the end of the PNA incubation, 0.5 g of soil/sediment slurry was collected from each
178 bottle in 2 ml RNase-free screw cap tubes and immediately flash-frozen in liquid N. Samples were
179 stored at -80°C upon DNA/RNA extraction.

180 RNPs were carried out at all sites in both bays as described by Taylor et al. (2010). Briefly, 5 g of
181 soil/wet sediments were added to 250 ml glass bottle containing 30 ml of PBS/site water amended

182 with 24 μM NaN_3 . Bottles were closed by butyl stoppers and 0.1% headspace acetylene gas (C_2H_2)
183 injected with a sterile syringe. C_2H_2 is an effective inhibitor of nitrification irreversibly blocking
184 archaeal and bacterial ammonia monooxygenase (AMO) enzyme. Bottles were incubated in the
185 dark for 3 h, after preliminary experiments showed this was sufficient time to inhibit the ammonia
186 monooxygenase (data not shown). C_2H_2 was removed by degassing for 10 min using a vacuum
187 pump. Butyl stoppers were removed to permit aeration and 250 μM NH_4^+ was added. Bottles were
188 then incubated for 72h (24 h to allow the synthesis of new AMO followed by a 48-h incubation).
189 Preliminary experiments showed that these conditions allowed efficient blocking and recovery
190 with high nitrification rates (data not shown). These settings in the absence of inhibitors were
191 considered the standard RNP. For all sites, two additional incubations were included: a) RNP with
192 50 μM ATU and 250 μM NH_4^+ ; b) RNP with 75 μM CHX and 250 μM NH_4 (see supplementary
193 Fig. S1). At the end of the 72 h incubation experiments, NO_2^- was extracted and measured as
194 indicated above. 0.5 g of soil/sediment slurry were collected from each bottle in 2 ml screw cap
195 tubes and immediately flash-frozen in liquid N for subsequent molecular analysis.

196 **DNA and RNA Co-Extraction**

197 DNA and RNA extractions from soils, sediments and soil/sediment slurries were carried out as
198 described by Tatti et al. (2016). Briefly, 0.5-0.7 g of fresh soil or sediment and 0.5 g soil/sediment
199 slurry were added to Lysing Matrix E tubes with 500 μl CTAB/Phosphate buffer and 500 μl
200 Phenol:Chloroform:Isoamyl alcohol (25:24:1) and vortexed at full speed for 2.5 minutes, followed
201 by centrifugation. The top layer was removed and added to 500 μl of Chloroform:Isoamyl alcohol
202 (24:1), mixed, and centrifuged. This was repeated, and the top layer was removed, and DNA/RNA
203 precipitated with two volumes of 30% PEG/1.6 M NaCl. Nucleic acids were pelleted by
204 centrifugation and re-suspended in 50 μl DEPC (diethylpyrocarbonate) water. A 30 μl aliquot of

205 DNA/RNA was removed to prepare RNA using TURBO DNase (Ambion, UK) according to the
206 manufacturer's instructions. The absence of DNA from the RNA fraction was confirmed by no
207 amplification of the 16S rRNA gene using primers F63 (5'-CAG GCC TAA CAC ATG GCA AGT
208 C-3') and 518R (5'-ATT ACC GCG GCT GCT GG-3') (Marchesi et al., 1998; Muyzer et al.,
209 1993). 2 µl of RNA template (undiluted, 10⁻¹ or 10⁻² dilution) were added to a 50 µl PCR mixture
210 containing 5 µl PCR buffer including MgCl₂ (Sigma Aldrich, Ireland), 0.2 mM of each
211 deoxynucleoside triphosphate (dNTP; Ambion, UK), 0.25 µM of each primer (Eurofins,
212 Germany), and 2.5 units of *Taq* polymerase (Sigma Aldrich, Ireland). The reaction was initially
213 denatured at 95°C for 5 min; followed by 30 cycles of 95°C for 30 s, 57°C for 30 s, and 72°C for
214 1 min; followed by a final extension step at 72°C for 7 min. The absence of a 16S rRNA gene band
215 was visually confirmed on a 1% agarose gel. DNA and RNA were quantified using Quant-iT™
216 DNA and RNA Assay Kits (ThermoFisher, UK) and Qubit fluorometer (Thermofisher, UK). DNA
217 and RNA were stored at -80°C until further analysis.

218 **cDNA Synthesis**

219 RNA was converted to cDNA using Superscript III (Life Science, USA). Gene specific reverse
220 transcription PCR (RT-PCR) amplification was performed on RNA targeting AOA and AOB
221 *amoA* transcripts. The initial RT reaction mixture contained 250 ng of RNA, 2 mM of the
222 appropriate reverse primer, archaeal *amoA616R* (GCC ATC CAT CTG TAT GTC CA, Tourna et
223 al., 2008) or bacterial *amoA2R* (CCC CTC KGS AAA GCC TTC TTC, Rotthauwe et al., 1997),
224 and 10 mM of each dNTP. The mixture was denatured at 65°C for 5 min and transferred to ice for
225 1 min. 5X first-strand buffer, 0.1 mM RNase Out (Thermo Fisher, UK), and 200 units SuperScript
226 III was added to the reaction mixture and incubated at 55°C for 50 min, followed by inactivation
227 of the reaction at 72°C for 10 min. Samples were stored at -80°C until further analysis.

228 **Quantitative PCR**

229 Archaeal and bacterial *amoA* genes (i.e., DNA) and transcripts (i.e., cDNA) were quantified by
230 qPCR from triplicate samples collected along the terrestrial-marine gradients. Triplicate no-
231 template controls (NTC) and appropriate standard curve were included in each assay. DNA/cDNA
232 extracts were tested for the presence of co-extracted inhibitory substances, as previously described
233 (Tatti et al., 2016). A 1:10 dilution was used to remove inhibitory substances (data not shown).
234 Quantitative PCR was performed using the SsoFast™ EvaGreen® master mix (Biorad, England),
235 archaeal *amoA* primers amoA23F (ATG GTC TGG CTW AGA CG) (Könneke et al., 2005) and
236 amoA616R (Tourna et al., 2008) at 200 nM each or bacterial *amoA* primers amoA1F (GGG GHT
237 TYT ACT GGT GGT) (Stephen et al., 1999) and amoA2R (CCC CTC BGS AAA VCC TTC TTC)
238 (Hornek et al., 2006) at 200 nM each, plus 1 ng of DNA/cDNA in a 20 µl reaction. These AOB
239 primers were selected for their higher coverage of AOB *amoA* (Hornek et al., 2006; Stephen et al
240 1999). Cycling conditions were: 1 cycle of 95°C for 5 min and then 40 cycles of 95°C for 30 s,
241 47°C AOB/ 55 °C AOA for 30 s, 72°C for 60 s. Fluorescence was measured at 82°C AOB/81°C
242 AOA. qPCR assays were conducted using Roche Lightcycler 480 (Roche). DNA and RNA
243 standard curves were constructed by amplifying the gene of interest according to Smith et al. 2006.
244 The standard curve descriptors for the abundance of nitrifiers communities were: for archaeal
245 *amoA* gene copy numbers/transcripts: slope = -2.97, Efficiency = 117.1%, $R^2 = 0.996$; for bacteria
246 *amoA* gene copy numbers/transcripts: slope = -3.03, Efficiency = 112.8%, $R^2 = 0.993$. Successful
247 amplification of the desired fragments was assessed by agarose gel, while specificity was checked
248 by melt curve analysis.

249 **Denaturing Gradient Gel Electrophoresis (DGGE) Analysis**

250 PCR for DGGE analysis was carried out on archaeal and bacterial *amoA* at DNA and cDNA levels
251 for all samples along the terrestrial-benthic gradient for both *in situ* and *in vitro* (PNA and RNP
252 assays). *amoA* genes were PCR-amplified for DGGE using 0.25 μ M amoA23f/amoA616r and
253 amoA1F/amoA2R primers without GC tail for archaea and bacteria, respectively and 2 U Taq
254 Polymerase (Sigma, Ireland). PCR conditions were as follows: 94°C for 3 min; 10X (94°C for 30
255 s; 62°C (AOB)/60°C (AOA) for 45 s; -0.5°C at 3°/s; 72°C for 1 min) 30 X (94°C for 30 s; 57°C
256 (AOB)/55°C (AOA) for 45 s; 72°C for 1 min) with a final elongation step 72°C for 10 min. Correct
257 size amplicons were checked by gel electrophoresis. DGGE was performed only on Rusheen bay
258 samples, as Clew bay cDNA samples did not lead to a satisfactory yield of amplicons for DGGE.
259 DGGE analysis was performed using a DCode Universal Mutation Detection System (Bio-Rad
260 Laboratories). PCR products were loaded onto a 6% polyacrylamide gel containing a 15-45% or
261 20-45% denaturant, for archaeal and bacterial *amoA*, respectively. The gel was run at 70 V for 15
262 h with a constant temperature of 60°C. The gel was removed from the electrophoresis tank and
263 stained with GelStar™ Nucleic Acid Gel Stain 10,000X (Fisher Scientific, Ireland) for 30 min and
264 washed in 1X TAE buffer for 5 min before taking the final picture under 300 nm UV light. Bands
265 exhibiting presence/absence or contrasting relative intensities between DGGE profiles of genes
266 and transcripts were excised from DGGE profiles. DNA bands were placed in water overnight at
267 -20°C and then used as templates for PCR targeting archaeal or bacterial *amoA*. Cloning of PCR
268 products was carried out using pGEM T-Easy vector and competent *Escherichia coli* JM109 cells
269 (Promega, Ireland). Clones obtained from each excised band excised were randomly selected and
270 subjected to PCR. A total of 25 bands were excised, 8 for archaeal and 17 for bacterial *amoA* and
271 sent for Sanger sequencing at Source Bioscience (Dublin, Ireland).

272 Clone sequences showing $\geq 99\%$ similarity were considered the same (Acinas et al., 2005).
273 Sequences were compared to sequences available in GenBank database
274 (<http://www.ncbi.nlm.nih.gov/>) and were then imported into Mega7 (Kumar et al., 2016) aligned
275 using Clustal W. Phylogenetic trees were constructed using the neighbor-joining method, and tree
276 topology was evaluated by bootstrap analysis. Sequences generated in this study have been
277 deposited in the GenBank database (Accession Numbers: MW369505 to MW369529).

278 **Statistical Analysis**

279 Graphpad PRISM was used to conduct statistical analyses (Graphpad Software Inc., La Jolla,
280 USA). Non-normal data were log-transformed. General linear model analysis of variance was
281 performed based on a completely randomized design with site, or site and microbial group (i.e.,
282 AOA/AOB), or site and potential plus ATU/CHX as fixed factor(s), for the physico-chemical
283 gradient characteristics, DNA/cDNA *amoA* qPCR quantification and PNA/RNP analysis,
284 respectively. Site, microbial group and potential plus ATU/CHX means were compared by a post
285 hoc Tukey honesty (HSD) test. Pearson's test (R^2 coefficient) was used to determine possible linear
286 relationships between the parameters: pH, NO_3 , NH_4^+ , DON, DOC, PNA, RNP, pH, archaeal and
287 bacterial *amoA* abundance and transcript levels and were considered significant from a two-tailed
288 test at $P < 0.05$.

289 Phoretix software (TotalLab Ltd, Newcastle-Upon-Tyne, UK) was used to obtain matrices from
290 DGGE profiles consisting of the relative intensity of each band (i.e., ratios of the intensity of each
291 band to the total band intensity). Similarities between the banding patterns generated by PCR-
292 DGGE of selected samples were analysed using Pearsons correlation coefficient and were

293 displayed as a dendrogram. Clustering algorithms were used to calculate the unweighted pair group
294 method with arithmetic averages (UPGMA).

295 Matrices were analysed using PRIMER v6 software (Plymouth, UK). Rank similarity matrices
296 were computed. The difference between *in situ* (DNA/RNA extracted from environmental
297 samples) and *in vitro* (DNA/RNA extracted from PNA/RNP samples) of bacterial and archaeal
298 ammonia oxidizing community structures was tested by Permutational Multivariate Analysis of
299 Variance (PERMANOVA).

300 **Results**

301 **Physico-Chemical Characteristics of the Soil-Sediment Gradient**

302 The two-chosen soil-sediment gradients showed similar chemical-physical characteristics (**Tab.**
303 **1**). Both bays presented an increasing gradient in pH from the soil to the marine site. In Rusheen
304 bay, the pH went from 7.2 in soil (e.g., Rsoil_1) to 8.5 in marine sandy site (Rsed_sand). In Clew
305 bay, the soil pH was slightly acidic (6.4 in Csoil) and then gradually increased to 8.9 in the marine
306 sandy site (Csed_sand). Similarly, salinity increased along the two gradients, ranging from 4.9-5.8
307 in the soil sites to 33.0-34.0 in marine sediments. In Clew bay, due to the input of freshwater from
308 a small natural stream, the gravelly sandy-muddy site (Csed_mix) had a salinity of 8.2 at the time
309 of sampling (low tide). Both bays generally showed low NO_3^- concentrations, ranging from $0.40 \pm$
310 0.14 to $2.26 \pm \text{SD}0.09 \mu\text{g N g}^{-1}$ soil/sediment. The muddy sites (Rsed_mud and Csed_mud) had the
311 highest values, while the sandy sites (Rsed_sand and Csed_mix) showed the lowest NO_3^-
312 concentration in each bay. Interestingly, NO_2^- concentration in Clew bay were higher than Rusheen
313 bay, where they ranged from 0.25 ± 0.04 (Csed_sand) to 2.05 ± 1.52 (Csed_mud) $\mu\text{g N g}^{-1}$
314 soil/sediment and were greater than NO_3^- concentrations in Cint and Csed_mix (1.82 ± 1.50) to

315 2.05±1.52 $\mu\text{g N g}^{-1}$ soil/sediment, respectively). In contrast NO_2^- was lower in Rusheen bay
316 ranging from 0.12±0.04 to 0.38±0.23 $\mu\text{g N g}^{-1}$ soil/sediment and always lower than the
317 corresponding site NO_3^- . The two bays showed different NH_4^+ , DOC and DON trends along their
318 soil-marine sites (**Tab. 1**). In Rusheen bay, NH_4^+ concentration ranged from 52.75±3.79 to
319 119.88±35.57 $\mu\text{g N g}^{-1}$ soil/sediment with the interface site (Rint) having the highest NH_4^+ values,
320 while the sandy site (Rsed_sand) showed the lowest NH_4^+ concentration. In Clew bay, the NH_4^+
321 concentration ranged from 33.55±8.06 to 118.42±65.73 $\mu\text{g N g}^{-1}$ soil/sediment, with the soil site
322 (Csoil) showing the lowest values and the interface site (Cint) having the highest. In Rusheen bay,
323 DOC concentration ranged from 60.4±0.97 to 92.55±3.12 $\mu\text{g C g}^{-1}$ soil/sediment and in Clew bay
324 from 51.61±5.40 to 149.17±1.56.

325 DON concentration ranged from 10.68±1.01 to 17.67±0.73 $\mu\text{g N g}^{-1}$ soil/sediment in Rusheen bay,
326 and from 11.5±3.01 to 24.3±1.96 $\mu\text{g N g}^{-1}$ soil/sediment in Clew bay. In Rusheen bay, soil, and
327 interface sites (Rsoil and Rint) showed the highest DOC/DON concentrations, while the marine
328 sandy site (Rsed_sand) had the lowest. In Clew bay, the muddy sediment site (Csed_mud) showed
329 the highest DOC/DON values, while the lowest concentrations of DOC/DON were measured in
330 soil and interface sites (Csoil and Cint).

331 **Abundance of Archaeal/Bacterial *amoA* Genes and Transcripts along the Gradient**

332 *amoA* genes were quantified from all sites. AOB ranged from $2.76 \times 10^5 \pm 2.67 \times 10^5$ Csoil to 7.65
333 $\times 10^7 \pm 3.02 \times 10^6$ Rsed_mud genes g^{-1} FW soil/sediment. AOA ranged from $2.8 \times 10^3 \pm 8.63 \times$
334 10^2 Rsed3 to $7.69 \times 10^7 \pm 1.64 \times 10^7$ Cint genes g^{-1} FW soil/sediment (**Fig 2**). In both bays,
335 sediment AOB *amoA* gene abundances were significantly greater than AOA *amoA* gene

336 **Table 1.** Chemico-physical characteristics of chosen sites in Rusheen (R) and Clew (C) bay. DOC: dissolved organic carbon. DON:
 337 dissolved organic nitrogen

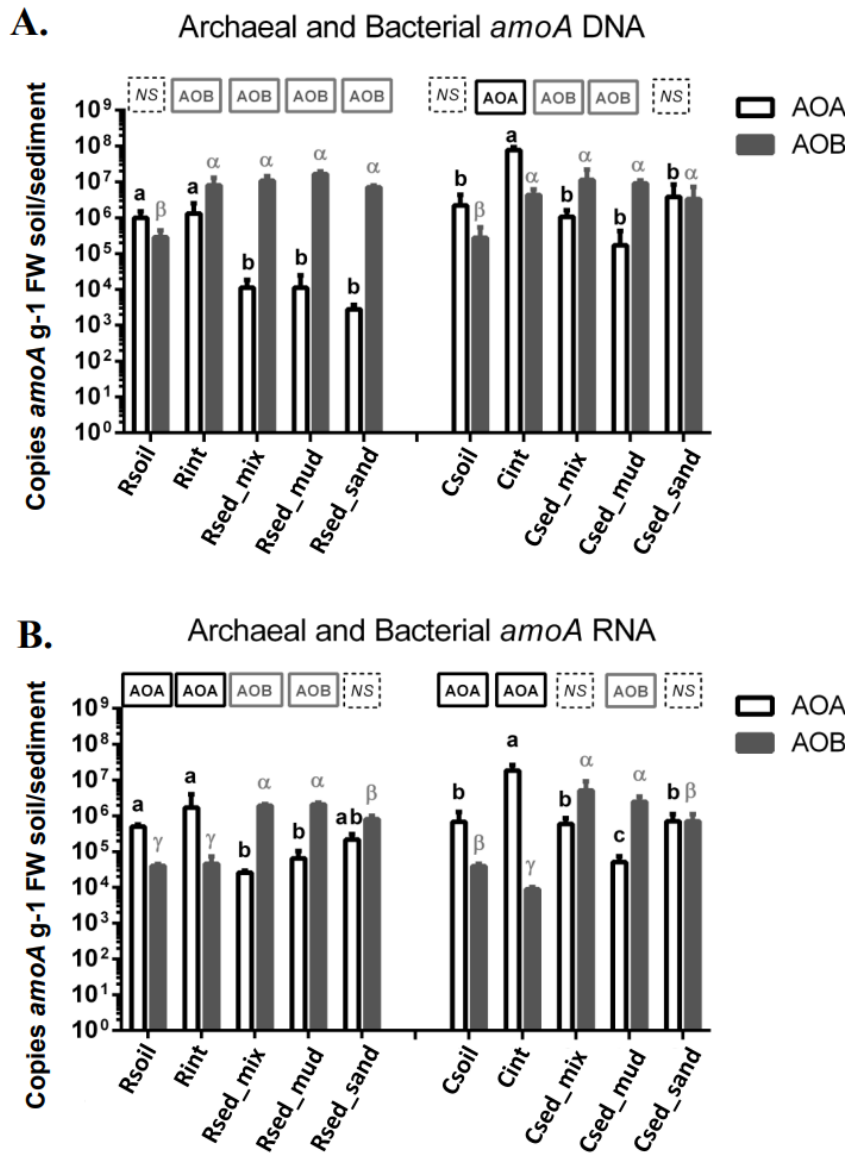
| Site | NO₃⁻ (µg N g ⁻¹) | NO₂⁻ (µg N g ⁻¹) | NH₄⁺ (µg N g ⁻¹) | pH | Salinity | DOC (µg C g ⁻¹) | DON (µg N g ⁻¹) | Classification |
|------------------|--|--|--|-----------------|-----------------|---------------------------------------|---------------------------------------|-----------------------|
| Rsoil | 1.37 (±0.13) | 0.30 (±0.13) | 104.88 (±21.8) | 7.18 (±0.14) | 5.77 | 82.89 (±6.22) | 15.46 (±1.85) | Soil |
| Rint | 1.71 (±0.39) | 0.38 (±0.23) | 119.9 (±35.57) | 7.71 (±0.1) | 15.34 | 89.02 (±18.31) | 17.67 (±0.73) | Interface |
| Rsed_mix | 1.01 (±0.08) | 0.31 (±0.16) | 67.45 (±7.3) | 8.2 (±0.14) | 30.04 | 72.35 (±9.11) | 12.32 (±0.28) | Muddy Sand |
| Rsed_mud | 1.51 (±0.06) | 0.36 (±0.04) | 82.36 (±8.01) | 8.15 (±0.04) | 33.01 | 92.55 (±3.12) | 13.67 (±1.22) | Muddy |
| Rsed_sand | 0.92 (±0.01) | 0.12 (±0.04) | 52.75 (±3.79) | 8.52 (±0.07) | 33.04 | 60.4 (±0.97) | 10.68 (±1.01) | Sand |
| Csoil | 2.26 (±0.09) | 1.47 (±0.24) | 33.55 (±8.06) | 6.42 (±0.33) | 4.86 | 77.79 (±38.53) | 19.38 (±1.93) | Soil |
| Cint | 1.46 (±0.59) | 1.82 (±1.5) | 118.42 (±65.73) | 7.26 (±0.68) | 13.11 | 51.61 (±5.40) | 15.28 (±4.8) | Interface |
| Csed_mix | 0.40 (±0.14) | 1.04 (±0.24) | 59.16 (±4.6) | 8.75 (±0.03) | 12.11 | 98.72 (±6.03) | 13.82 (±0.46) | Gravelly Muddy Sand |
| Csed_mud | 2.16 (±0.60) | 2.05 (±1.52) | 108.35 (±14.35) | 8.13 (±0.07) | 23.05 | 149.17 (±1.56) | 24.3 (±1.96) | Muddy |
| Csed_sand | 0.82 (±0.07) | 0.25 (±0.04) | 55.43 (±3.73) | 8.89 (±0.12) | 34.01 | 56.5 (±32.75) | 11.15 (±3.01) | Sand |

338

339 abundances at all sites except for Csed_sand ($P < 0.05$). For soil sites, AOA *amoA* gene abundances
340 were higher than AOB, although not significantly different. For the interface sites, at Rint, AOB
341 *amoA* gene abundances were significantly greater than AOA. At Cint, AOA *amoA* gene
342 abundances dominated and were significantly greater than those in both soil and sediment sites
343 ($P < 0.05$).

344 At mRNA level, *amoA* transcripts were quantified from all sites. AOB ranged from $8.87 \times 10^3 \pm$
345 1.5×10^3 Cint1 to $5.14 \times 10^6 \pm 4.13 \times 10^6$ Csed_mix transcripts g^{-1} FW soil/sediment. AOA ranged
346 from $1.1 \times 10^4 \pm 7.42 \times 10^3$ Rsed_mud to $7.69 \times 10^7 \pm 1.64 \times 10^7$, Cint transcripts g^{-1} FW
347 soil/sediment (**Fig 2B**). AOB transcripts were highest in the sediments, as observed for *amoA*
348 genes. However, there was no significant difference between AOA and AOB *amoA* gene transcript
349 abundances among the three sediment sites (Rsed_sand, Csed_mix and Csed_sand). AOA
350 transcripts dominated both soil and interface sites.

351 AOB *amoA* gene abundances in both bays were positively correlated with pH and salinity
352 (Pearson's correlation, $P < 0.05$) and with NH_4^+ in Clew Bay only (0.71, $P < 0.003$) (**Tab. 2**). AOA
353 *amoA* gene abundances in Rusheen Bay were positively correlated with NH_4^+ , DON and DOC
354 (0.853, $P < 0.0003$; 0.763, $P < 0.0005$; 0.747, $P < 0.001$, respectively), but negatively with salinity (-
355 0.811, $P < 0.0004$). AOA *amoA* gene abundances from Clew bay did not correlate with any of the
356 measured physical-chemical variables



357

358 **Figure 2.** Abundance of AOA and AOB *amoA* gene (A) and transcript (B) across Rusheen and
 359 Clew bays. Values are mean (n=3) and error bars are standard error. One-way ANOVA and Tukey
 360 post-hoc test were used to test for statistical difference in gene or transcript abundances for AOA
 361 (denoted by standard letters) and AOB (denoted by Greek letter) within a bay. Within a site,
 362 statistical differences in gene or transcript abundance between AOA and AOB are indicated in the
 363 box on top of the bars, showing the dominant group. NS indicated no significant difference.

364 **Table 2.** Pearson correlations between the AOA and AOB abundance of *amoA* gene and transcripts, physico-chemical parameters and
 365 Potential Nitrification Activity (PNA) and Recovery of Nitrification Potential (RNP) in Rusheen and Clew bays. Only statistically
 366 significant results are shown, P<0.05 (*), P<0.01 (**), and P<0.001 (***). NS is non-significant.

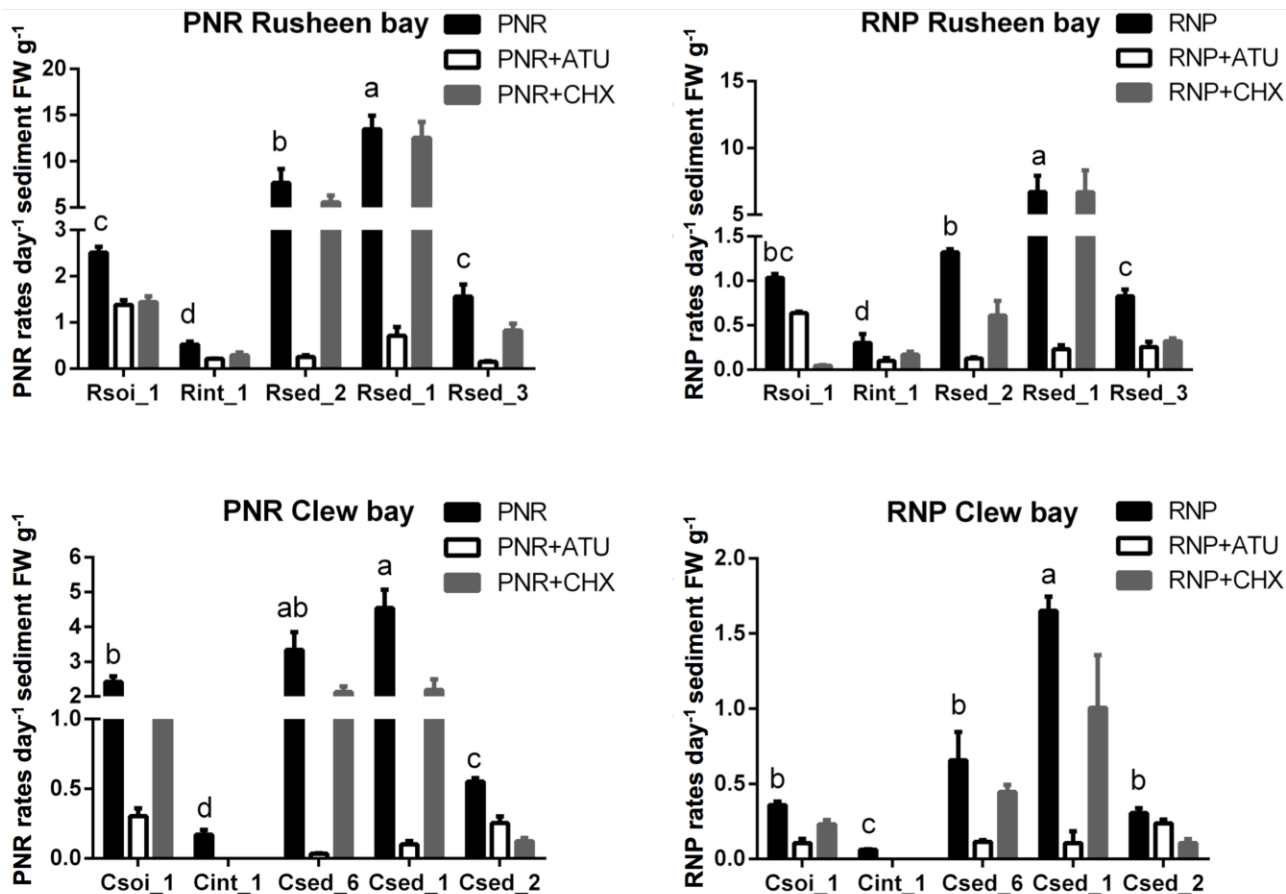
| | NO_3^- | NO_2^- | NH_4^+ | pH | DON | Salinity | DOC | PNA | RNP |
|---------------------|-----------------|-----------------|-----------------|--------------|-------------|--------------|-------------|--------------|--------------|
| Rusheen bay | | | | | | | | | |
| <i>amoA</i> AOB | NS | NS | NS | 0.569 (*) | NS | 0.744 (*) | NS | 0.623 (*) | NS |
| <i>amoA</i> AOA | 0.627 (*) | NS | 0.853 (***) | -0.797 (***) | 0.763 (***) | -0.811 (***) | 0.747 (**) | -0.523 (*) | NS |
| <i>amoA</i> AOB RNA | NS | NS | 0.809 (***) | 0.729 (*) | -0.746 (**) | 0.825 (**) | -0.645 (**) | 0.702 (**) | 0.617 (*) |
| <i>amoA</i> AOA RNA | 0.528 (*) | NS | 0.532 (*) | NS | 0.545 (*) | -0.574 (*) | NS | -0.719 (**) | -0.645 (*) |
| Clew bay | | | | | | | | | |
| <i>amoA</i> AOB | NS | NS | 0.709 (**) | 0.618 (*) | NS | 0.435 (*) | NS | 0.033 | NS |
| <i>amoA</i> AOA | NS | NS | NS | NS | NS | NS | NS | -0.831 (***) | -0.859 (***) |
| <i>amoA</i> AOB RNA | 0.555 (*) | NS | NS | 0.717 (**) | NS | NS | NS | 0.641 (*) | 0.739 (**) |

367

368 AOB transcripts from both bays had a strong positive correlation with pH (Rusheen, 0.729,
369 $P < 0.002$; Clew 0.722, $P < 0.003$) (**Tab. 2**). In Clew bay, AOB transcripts were positively correlated
370 with NO_3^- (0.555, $P < 0.043$). In Rusheen bay, AOB transcript were positively correlated with NH_4^+ ,
371 pH and salinity (but negatively correlated with DON (-0.746, $P < 0.001$) and DOC (-0.645,
372 $P < 0.0094$) (**Tab. S1**). In addition, AOA transcripts were positively correlated with NO_3^- , NH_4^+
373 and DON. pH and salinity were positively correlated ($R = 0.95$, $P < 0.05$) in both Rusheen and Clew
374 bays ($R = 0.55$, $P < 0.05$) (**Tab. S1**).

375 **PNA/RNP along the Gradient**

376 In Rusheen bay, PNAs ranged from 0.7 to 14.5 $\text{day}^{-1} \text{g}^{-1}$ FW sediment/soil (**Fig. 3A**). The highest
377 rates were measured in Rsed_mud, while the lowest were in Rint. With the addition of inhibitors
378 (ATU, mostly bacteria; CHX, mostly archaea), there was no significant difference between the
379 contribution of ATU- or CHX-sensitive AO at the Rsoil and Rint sites. On the other hand, ATU-
380 sensitive AO was significantly inhibited in the marine sites Rsed_mix, and Rsed_sand. RNP,
381 following C_2H_2 inactivation of AMO, ranged from 0.3 to 6.1 $\text{day}^{-1} \text{g}^{-1}$ FW sediment/soil (**Fig. 3B**),
382 which were significantly lower than the PNAs. Highest and lowest RNPs were measured in
383 Rsed_mud and Rint, respectively. With the addition of inhibitors, CHX-sensitive AO was
384 significantly reduced compared to ATU-sensitive AO in Rsoil, while in Rsed_mix and Rsed_mud
385 ATU-sensitive AO was significantly reduced. There was no significant difference between CHX
386 and ATU-sensitive AO in Rint and Rsed_sand.



387

388 **Figure 3. Potential Nitrification Activity (PNA) and Recovery of Nitrification Potential (RNP) rates across Rusheen and Clew**
 389 **bay.** Values are mean (n=3) and error bars are standard error. Changes in PNA (A and C; black bars) and RNP (B and D; black
 390 bars) across the bay were tested using one-way ANOVA and Tukey post hoc test. Statistically significant differences are
 391 represented by standard letters on top of the bars.

392 In Clew bay, PNAs were between 0.25 and 4.6 day⁻¹ g⁻¹ FW sediment/soil, which were lower than
393 those observed in Rusheen bay (**Fig 3C**). The highest rates were measured in Csed_mud and lowest
394 in Cint. With the addition of inhibitors, ATU-sensitive AO was significantly reduced in Csoil,
395 Csed_mix and Csed_mud. No significant difference was detected between CHX- and ATU-
396 sensitive AO in Csed_sand. Despite several optimization attempts, no PNAs were measured from
397 the Cint site when inhibitors were used. RNPs rates ranged from 0.15 to 1.6 day⁻¹ g⁻¹ FW
398 sediment/soil, significantly lower compared to PNAs. When ATU and CHX were used, ATU-
399 sensitive AO was dominant over CHX-sensitive AO in both Csed_mix and Csed_mud. No
400 significant difference was measured in the contribution of ATU- or CHX-sensitive ammonia
401 oxidation in Csoil and Csed_sand. Moreover, no RNPs were measured in Cint when inhibitors
402 were used.

403 In Rusheen bay, PNA positively correlated with AOB *amoA* genes (0.623, P<0.01) and transcripts
404 (0.702, P<0.003) but negatively with AOA *amoA* genes (-0.523, P<0.045) and transcripts (-0.719,
405 P<0.002) (**Tab. 2**). While no significant correlation was observed between AOB *amoA* genes and
406 RNP, there was a strong positive correlation at transcription level (0.617, P<0.0018). In contrast,
407 AOA *amoA* transcripts negatively correlated with RNP (-0.645, P<0.012). In Clew bay, AOB
408 *amoA* transcripts positively correlated with PNA (0.641, P<0.01) and RNP (0.739, P<0.002) while
409 both AOA *amoA* genes and transcripts negatively correlated with PNA and RNP (**Tab. 2**).

410 **PNA/RNP versus *in situ* Active Nitrifier Community Structure**

411 Analysis of *amoA* transcript structure *in situ* and within PNA and RNP assays was carried out for
412 soil and sediment sites in Rusheen bay only (Fig. 4). Sufficient transcripts were not recovered from

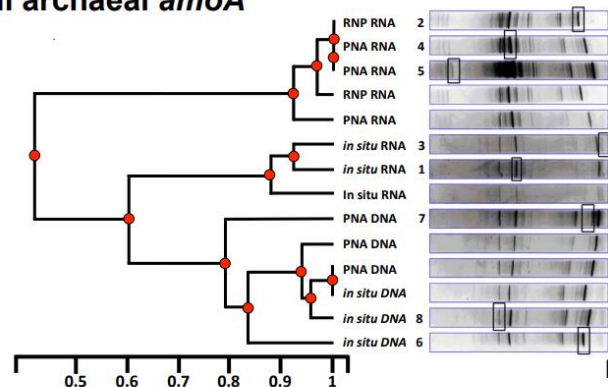
413 Rint or any of the Clew Bay sites for DGGE analysis. For Rsoil, only archaeal *amoA* was recovered
414 (Fig 4A) and analysed by DGGE. While for, Rsed_mix (Fig 4B), Rsed_mud (Fig 4C) and
415 Rsed_sand (Fig 4B), bacterial *amoA* but not archaeal *amoA* transcripts were recovered and
416 analysed by DGGE.

417 In the Rsoil site for AOA (at DNA level), the *in situ* and PNA profiles were similar ($P < 0.775$) and
418 the same number of bands were detected in both ($n = 11 \pm 1$) (**Fig. 4A**). However, at RNA level, *in*
419 *situ* was significantly different to PNA ($P < 0.023$), with less bands *in situ* ($n = 9 \pm 1$) than in the PNA
420 ($n = 17 \pm 2$), and a Jaccard similarity of only 43%. Both PNA and RNP RNA profiles were similar
421 ($P < 0.901$) and had the same number of bands (**Fig. 4A**).

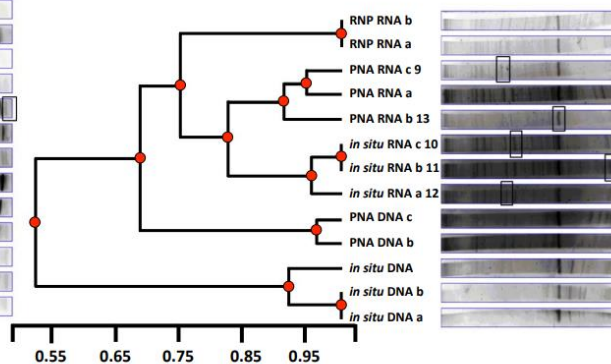
422 In Rsed_mix for AOB (at DNA level), *in situ* and PNA profiles were significantly different
423 ($P < 0.017$), the PNA community had 14 ± 1 distinct bands and the RNP 8 ± 2 (**Fig. 4B**). However, at
424 RNA level, *in situ* and the PNA AOB community were similar ($P < 0.389$), with a similar number
425 of bands in both ($n = 18 \pm 0.3$, PNA; $n = 19 \pm 0.5$, *in situ*) and a 83% Jaccard similarity index. The
426 transcripts from the RNP were significantly different in both community structure and number of
427 detected bands ($n = 16 \pm 2$, Fig 3B), to that in the PNA and *in situ*.

428 In Rsed_mud, for AOB at DNA level the *in situ* and PNA profiles were significantly different
429 ($P < 0.042$) with 4 ± 1 bands PNA and 2 *in situ* (**Fig. 3C**). However, at the RNA level, *in situ* and
430 PNA profiles were far more diverse and more similar to each other ($P < 0.17$), with 24 ± 1.5 *in situ*
431 and 23 ± 2 PNA detected bands, respectively, and a Jaccard index of similarity of 86% (**Fig. 4C**).
432 Since corresponding DNA bands were not observed in the DNA DGGE (red rectangles **Fig. 4C**),
433 this indicates the presence of a low abundant but highly transcriptionally active group of AOB at

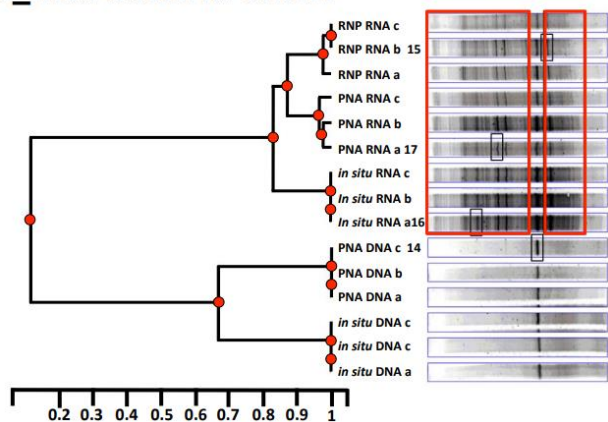
A. Rsoil archaeal *amoA*



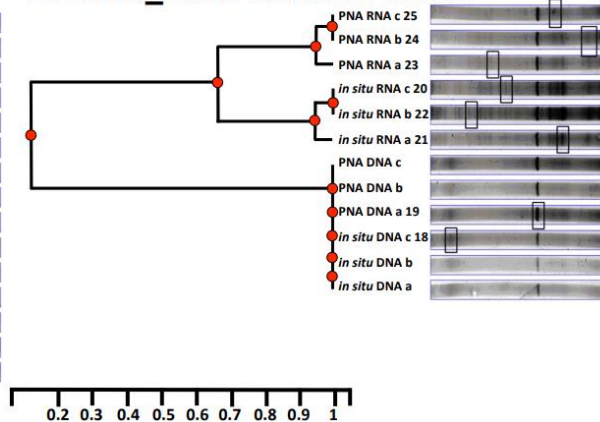
B. Rsed_mix bacterial *amoA*



C. Rsed_mud bacterial *amoA*



D. Rsed_sand bacterial *amoA*



434

435 **Figure 4.** UPGMA-based dendrograms of DNA and RNA *amoA* community in PNA/RNP and *in situ* obtained by DGGE profiles for

436 the analyzed sites in Rusheen bay. Bands indicated by box and number were excised and sequenced for taxonomic/phylogenetic analysis.

437 Red rectangles in Figure 4C indicate AOB members low in abundance but highly active. Scale on the X axis represent the distance

438 between samples (percentage dissimilarity) based on the banding pattern.

439 this site (**Fig 4C**). There was no significant difference ($P < 0.722$) between the PNA and RNP RNA
440 profiles.

441 In Rsed_sand for AOB (at the DNA level) the *in situ* and PNA profiles were similar ($P < 0.832$)
442 with two dominant bands. However, *in situ* and PNA profiles were more similar at RNA level than
443 DNA profile, with 12 ± 1 bands *in situ* and 8 ± 1 on the PNA, and a Jaccard similarity of 69%. No
444 amplification of *amoA* transcripts from RNP samples was obtained.

445 Some of the active ammonia oxidizers from *in situ* PNA and RNP conditions were identified
446 following the excision and sequencing of dominant DGGE bands (Fig 4). Eight and seventeen
447 bands were obtained from archaeal and bacterial *amoA* respectively. *amoA* sequences were
448 generally more similar to sequence from uncultured representatives than from isolated strains
449 (**Figs. S1** and **S2**). Bacterial *amoA* sequences grouped in a single cluster most similar to the known
450 *Nitrosomonas* and uncultured *amoA* from similar marine/estuarine/salt marsh sediments (**Fig. S1**).
451 The archaeal *amoA* sequences (Rsoil DGGE 1-3, Rsoil DGGE 5-8) belonged to Group I.1a along
452 with uncultured sequences from similar sediment/soil environments (**Fig. S2**). Only one sequence,
453 Rsoil DGGE 4 belonged to Group I.1b clustering with *amoA* sequences obtained from other soil
454 environments.

455 **Discussion**

456 In the present work, we measured the abundance and transcriptional activity of ammonia oxidizers
457 along soil-sediment gradients in two coastal bays. The sediment and soil environments showed
458 differences in the abundance and transcriptional activity of the nitrifying communities. Gene and
459 transcript quantification showed the dominance of AOB in sediments (**Fig. 2**), while AOA

460 transcripts were more abundant in soil and interface samples from both bays (**Fig 2**). pH and
461 salinity were key drivers separating AOA and AOB across the gradient (**Tab. 1 & 2**).

462 We further investigated the suggested trend from the molecular data on the contribution of AOA
463 and AOB to PNA/RNP using selective inhibitors. The use of inhibitors has shortcomings, with
464 some AOB insensitive to ATU (Lehtovirta-Morley et al., 2013; Shen et al., 2013) and some AOA
465 insensitive to cycloheximide (Taylor et al, 2010; Wright et al., 2020). This means that they cannot
466 be assumed to reliably inhibit only AOA or AOB. They were selected at the time of the experiment
467 as the best inhibitors, but there have since been further developments, in particular for AOA, such
468 as the use of 2-phenyl-4, 4, 5, 5, -tetramethylimidazoline-1-oxyl 3-oxide (PTIO) (Huang et al.,
469 2021). However, use of the selected inhibitors in combination with the transcript data from this
470 work, and that of our previous work (Zhang et al., 2018), adds to the evidence and supports the
471 finding that AOA are the main contributor to AO in the soil sites while AOB are the main
472 contributor in marine sediments.

473 Exploiting this functional shift in AO, this work has shown that the experimental conditions used
474 during the measurement of nitrification potentials may lead to the response of different AO from
475 those active *in situ*, which may result in an altered view of the nitrification capability. Specifically,
476 the incubation conditions appear to be more suited to AOB than AOA. By targeting
477 transcriptionally active AOB we showed a similar community structure within the PNA/RNP
478 incubations and *in situ* for the mud and muddy-sandy sediment sites (Jaccard similarity values
479 83%, $P < 0.17$ and 86%, $P < 0.389$ respectively) (**Fig. 4**). Further sequencing would be required to
480 determine if these were the exact same AO. However, these findings support our hypothesis that
481 the PNA/RNP conditions did not adversely affect AOB activity and supports the high positive
482 correlations observed between AOB transcript abundance and measured PNA/RNP potentials in

483 from most AOB dominated sites (**Tab. 2**). In addition to the active *in situ* and PNA/RNP
484 communities being similar for AOB, we showed that there were more DGGE bands in the RNA
485 compared to DNA and a clear separate clustering of DNA and RNA (**Fig. 4C**). This indicates that
486 there are members within the AOB community that are low in abundance (DNA DGGE) but highly
487 active both *in situ* and in the PNA/RNA experiments (**Fig 4**). This result is consistent with Zhang
488 et al. (2018) who found a higher number of bands in the RNA DGGE compared to DNA DGGE
489 and with Duff et al. (2017) who found AOB OTUs present in cDNA but not DNA clone libraries
490 from muddy sediments. In this study, the sequencing of bands that were found only in the RNA
491 revealed that they were affiliated to unknown β -proteobacteria. Future studies should focus on
492 identifying these unknown transcriptionally active AOB that likely drive ammonia oxidation in
493 sediments, for example through DNA/RNA SIP to label and target active nitrifiers.

494 For AOA we showed that the incubation conditions did not select for the same active AOA
495 community as *in situ*, with a low level of similarity (43%) between active AOA *in situ* and
496 PNA/RNP community structure for the soil site (**Fig. 4**). For all soil and interphase sites, AOA
497 transcripts were greater than AOB (**Fig. 2**), yet the most striking example of inconsistencies
498 between transcripts abundance and potential rates was observed at the interphase soil/sediment. At
499 these sites the highest AOA *amoA* transcripts were recorded but no PNA/RNP was measured
500 despite extensive optimization efforts. Previously we have shown that both AOA and AOB were
501 contributing to nitrification in the soil/sediment interface (Zhang et al., 2018), and this may explain
502 why it was difficult to optimize PNA for both groups. Other authors have indicated transition zones
503 between terrestrial and aquatic ecosystems as hot-spots for biogeochemical processes, since they
504 are crossed by both terrestrial and marine fluxes of nutrients, in particular the oxidized and reduced
505 forms of N (McClain et al., 2003; Zhu et al., 2013). Further investigations in different locations

506 are needed to clarify nitrification dynamics in interface sites between terrestrial and marine
507 environments. Indeed, at sites the use of RT-Q-PCR was a better indicator of AO activity than the
508 PNA/RNP, with the added advantage of the ability to distinguish between AOA and AOB.

509 Although an overall negative correlation was observed between AOA transcript abundance and
510 PNA/RNP (**Tab. 2**), rather than conclude that AOA are not active in the soil/interphase *is situ*, we
511 suggest that standard PNA/RNP incubation conditions are not favoring the resident active AOA.
512 This could be due to the excess of inorganic ammonia, O₂, agitation or homogenization used in the
513 assays. Further the AO from these sites may prefer other N sources rather than NH₄⁺ provided, for
514 example from cyanate (Palatinszky et al., 2015). Indeed, investigations of niche separation in soil
515 have shown the preferential activity of AOA when ammonia is supplied via mineralisation of
516 organic matter (Aigle et al., 2020). In this study, we found a positive and significant correlation
517 between AOA *amoA* transcript abundance and DON in Rusheen bay (**Tab. 2**) which could indicate
518 that AOA may use DON-derived ammonia in this environment. A recent review by Hazard et al.
519 (2021) showed that of 107 studies only 36% reported a significant positive correlation between
520 PNA and AOA gene abundance in soils and sediments verses 75% of studies showing a positive
521 correlation for AOB. They argued that instead of concluding that AOA is not active, as is often the
522 case, this low correlation is due to the inappropriate PNA incubation conditions that will differently
523 affect AOA and AOB. Indeed, PNA is not only affected by nitrifier abundances but also by
524 community composition (Hazard et al., 2021) which implies that physiological diversity within
525 communities will require bespoke incubation conditions for different groups of AO. This work
526 supports those conclusions.

527 **Conclusions**

528 Our study investigated the distribution, activity and dominance of AO across transition zones
529 between terrestrial (soil) and marine (sediment) environments. Gene and transcript data indicated
530 that AOA dominated in soil and interphase and AOB dominated in marine muddy sediments. For
531 AOB, a higher correlation was observed between PNA/RNP and transcript abundance compared
532 to DNA. Furthermore, RNA DGGE revealed the presence of active AOB *in situ* and in the PNA
533 experiment that were of too low abundance to be detected in the DNA DGGE. Interestingly, we
534 show that PNA/RNP analyses may provide a good picture of the environmental nitrification
535 capacity when AOB are the dominant group, with the same transcripts present at the end of
536 PNA/RNP incubation and detected *in situ*. On the other hand, negative correlations between AOA
537 transcript abundance and PNA/RNP were observed, indicating that incubation conditions used in
538 this study did not favor the resident active AOA. This supports our hypothesis that PNA is suited
539 to reflect AOB but not AOA activity.

540 **Declaration of competing interest**

541 We have no conflicts of interest to declare.

542 **Acknowledgements**

543 Authors would like to thank Agata Lisik for her invaluable help during soil and sediment sampling
544 in Rusheen and Clew bays. Dr. Ciara Keating for kind assistance with DGGE. This work was
545 supported by an SFI SIRG award (11/SIRG/B2159) to CJS “Molecular Ecology of Ammonia
546 Oxidation in Coastal Sediments, funding ET and AD. CJS is currently supported by a Royal
547 Academy of Engineering-Scottish Water Research Chair (RCSRF1718643). UIJ is supported by
548 NERC IRF NE/L011956/1.

549 **Credit Authorship Contribution Statement**

550 **ET:** Conceptualization; Investigation, Methodology; Writing - original draft; **AMD:**
551 Conceptualization, Writing - review & editing. **AK** and **FC:** Writing – review and editing; **UZI:**
552 Visualization, Software; **CJS** Conceptualization; Methodology, Writing; Supervision, Resources,
553 Funding acquisition.

554 **References**

555 Acinas, S.G., Sarma-Rupavtarm, R., Klepac-Ceraj, V., Polz, M.F. (2005). PCR-induced sequence
556 artifacts and bias: insights from comparison of two *16S rRNA* clone libraries constructed from the
557 same samples. *Appl. Environ. Microbiol.* 71, 8966-8969. doi: 10.1128/AEM.71.12.8966-
558 8969.2005

559 Agogu e, H., Brink, M., Dinasquet, J., and Herndl, G.J. (2008). Major gradients in putatively
560 nitrifying and non- nitrifying Archaea in the deep North Atlantic. *Nature* 456, 788-91. doi:
561 10.1038/nature07535

562 Aigle, A., Gubry-Rangin, C., Thion, C., Estera-Molina, K.Y., Richmond, H., Pett-Ridge, J.,
563 Firestone, M.K., Nicol, G.W., Prosser, J.I. (2020). Experimental testing of hypotheses for
564 temperature- and pH-based niche specialization of ammonia oxidizing archaea and bacteria.
565 *Environ. Microbiol.* 22, 4032-4045. doi: 10.1111/1462-2920.15192

566 Bai, Y., Sun, Q., Wen, D., Tang, X. (2012). Abundance of ammonia-oxidizing bacteria and archaea
567 in industrial and domestic wastewater treatment systems. *FEMS Microbiol. Ecol.* 80, 323-330. doi:
568 10.1111/j.1574-6941.2012.01296.x

569 Bollmann, A., French, E., Laanbroek, H.J. (2011). Oxidizing bacteria and archaea adapted to low
570 ammonium concentration. *Meth. Enzymol.* 486, 55-88. doi: 10.1016/S0076-6879(11)86003-9

571 Cao, H., Hong, Y., Li, M., and Gu, J.D. (2011). Diversity and abundance of ammonia-oxidizing
572 prokaryotes in sediments from the coastal Pearl River estuary to the South China Sea. *Antonie van*
573 *Leeuwenhoek, Int. J.* 100, 545-456. doi: 10.1007/s10482-011-9610-1

574 Daims, H., Lebedeva, E.V., Pjevac, P., Han, P., Herbold, C., Albertsen, M., Jehmlich, N.,
575 Palatinszky, M., Vierheilig, J., Bulaev, A., Kirkegaard, R.H., von Bergen, M., Rattei, T.,
576 Bendinger, B., Nielsen, P.H., Wagner, M. (2015). Complete nitrification by *Nitrospira* bacteria.
577 Nature. 528, 504-509. doi: 10.1038/nature16461

578 Di, H.J., Cameron, K.C., Shen, J.P., Winefield, C.S., Ocallaghan, M., Bowatte, S., He, J.Z. (2009).
579 Nitrification driven by bacteria and not archaea in nitrogen-rich grassland soils. Nat. Geosci. 2:9,
580 621-624. doi: 10.1038/ngeo613

581 Di, H.J., Cameron, K.C., Shen, J.P., Winefield, C.S., O'Callaghan, M., Bowatte, S., He, J.Z.
582 (2010). Ammonia-oxidizing bacteria and archaea grow under contrasting soil nitrogen conditions.
583 FEMS Microbiol. Ecol. 72, 386-394. doi: 10.1111/j.1574-6941.2010.00861.x

584 Duff, A.M., Zhang, L.-M., Smith, C.J. (2017). Small-scale variation of ammonia oxidisers within
585 intertidal sediments dominated by ammonia-oxidising bacteria *Nitrosomonas sp. amoA* genes and
586 transcripts. Sci. Rep. 7:1, art. no. 13200. doi: 10.1038/s41598-017-13583-x

587 Fernandes, S.O., Javanaud, C., Michotey, V.D., Guasco, S., Anschutz, P., Bonin, P. (2016).
588 Coupling of bacterial nitrification with denitrification and anammox supports N removal in
589 intertidal sediments (Arcachon Bay, France). Estuar. Coast. Shelf Sci. 179, 39-50. doi:
590 10.1016/j.ecss.2015.10.009

591 Francis, C.A., Roberts, K.J., Beman, J.M., Santoro, A.E., and Oakley, B.B. (2005). Ubiquity and
592 diversity of ammonia-oxidizing archaea in water columns and sediments of the ocean. Proc. Natl.
593 Acad. Sci. U. S. A. 102, 14683-14688. doi: 10.1073/pnas.0506625102

594 Gruber, N., Galloway, J. N. (2008). An Earth-system perspective of the global nitrogen cycle.
595 *Nature*. 45, 293-296. doi: 10.1038/nature06592

596 Gubry-Rangin, C., Nicol, G.W., Prosser, J.I. (2010). Archea rather than bacteria control
597 nitrification in two agricultural acidic soils. *FEMS Microbiol. Ecol.* 74, 566-574.
598 doi:10.1111/j.1574-6941.2010.00971.x

599 Hart, S.C., Stark, J.M., Davidson, E.A., Firestone, M.K. (1994). Nitrogen mineralization,
600 immobilisation and nitrification. In: Weaver, R.W., Angle, J.S., Bottomley, P.S. (Eds.), *Methods*
601 *of Soil Analysis. Part 2. Microbial and Biogeochemical Properties*. SSSA, Madison, 985–1018.
602 doi: 10.1128/aem.59.7.2093-2098.1993

603 Hazard, C., Prosser, J.I., Nicol, G. W. (2021). Use and abuse of potential rates in soil microbiology.
604 *Soil Biol. Biochem.* 157, art. no. 108242, . doi: 10.1016/j.soilbio.2021.108242

605 Hink, L., Nicol, G.W., and Prosser, J.I. (2017). Archaea produce lower yields of N₂O than bacteria
606 during aerobic ammonia oxidation in soil. *Environ. Microbiol.* 19, 4829-4837. doi: 10.1111/1462-
607 2920.13282

608 Hink, L., Gubry-Rangin, C., Nicol, G.W., Prosser, J.I. (2018). The consequences of niche and
609 physiological differentiation of archaeal and bacterial ammonia oxidisers for nitrous oxide
610 emissions. *ISME J.* 12, 1084-1093. doi: 10.1038/s41396-017-0025-5

611 Hornek, R., Pommerening-Röser, A., Koops, H.P., Farnleitner, A.H., Kreuzinger, N., Kirschner,
612 A., and Mach, R.L. (2006). Primers containing universal bases reduce multiple amoA gene specific
613 DGGE band patterns when analysing the diversity of beta- ammonia oxidizers in the environment.
614 *J. Microbiol. Methods.* 6, 147-155. doi: 10.1016/j.mimet.2005.11.001

615 Huang, L., Chakrabarti, S., Cooper, J. et al. Perez, A., John, S. M., Daroub, S. H., Martens-
616 Habbena, W. (2021). Ammonia-oxidizing archaea are integral to nitrogen cycling in a highly
617 fertile agricultural soil. *ISME COMMUN.* 1, 19. doi: 10.1038/s43705-021-00020-4

618 Hyman, M. R., P. M. Wood. (1985). Suicidal inactivation and labeling of ammonia
619 monooxygenase by acetylene. *Biochem. J.* 227, 719-725.

620 Jäntti, H., Ward, B.B., Dippner, J.W., Hietanen, S. (2018). Nitrification and the ammonia-
621 oxidizing communities in the central Baltic Sea water column. *Estuar. Coast. Shelf Sci.* 202, 280-
622 289. doi: 10.1016/j.ecss.2018.01.019

623 Kits, K.D., Sedlacek, C.J., Lebedeva, E. V., Han, P., Bulaev, A., Pjevac, P., Daebeler, A., Romano,
624 S., Albertsen, M., Stein, L.Y., Daims, H., Wagner, M. (2017). Kinetic analysis of a complete
625 nitrifier reveals an oligotrophic lifestyle. *Nature* 549, 269-272. doi: 10.1038/nature23679

626 Kitzing, K., Marchant, H.K., Bristow, L.A., Herbold, C.W., Padilla, C.C., Kidane, A.T.,
627 Littmann, S., Daims, H., Pjevac, P., Stewart, F.J., Wagner, M., Kuypers, M.M.M. (2020). Single
628 cell analyses reveal contrasting life strategies of the two main nitrifiers in the ocean. *Nat. Commun.*
629 11,767, doi: 10.1038/s41467-020-14542-3

630 Könneke, M., Bernhard, A.E., De La Torre, J.R., Walker, C.B., Waterbury, J.B., Stahl, D.A.
631 (2005). Isolation of an autotrophic ammonia-oxidizing marine archaeon. *Nature.* 437, 543-546.
632 doi: 10.1038/nature03911

633 Koper, T.E., Stark, J.M., Habteselassie, M.Y., Norton, J.M. (2010). Nitrification exhibits Haldane
634 kinetics in an agricultural soil treated with ammonium sulfate or dairy-waste compost. *FEMS*
635 *Microbiol. Ecol.* 7:2, 316-322. doi: 10.1111/j.1574-6941.2010.00960.x

636 Kumar, S., Stecher, G., Takamura, K. (2016). Mega7: molecular evolutionary genetics analysis
637 version 7.0 bigger datasets. *Mol. Biol. Evol.* 33, 1870-74. doi: 10.1093/molbev/msw054

638 Kumwimba, MN., Meng, F. (2019). Roles of ammonia-oxidizing bacteria in improving
639 metabolism and cometabolism of trace organic chemicals in biological wastewater treatment
640 processes: A review. *Sci. Total Environ.* 659, 419-441. doi: 10.1016/j.scitotenv.2018.12.236

641 Lehtovirta-Morley, L.E., Verhamme, D.T., Nicol, G.W., Prosser, J.I. (2013). Effect of nitrification
642 inhibitors on the growth and activity of *Nitrosotalea devanaterra* in culture and soil. *Soil Biol
643 Biochem* 62, 129-133. doi: 10.1016/j.soilbio.2013.01.020

644 Li, H., Weng, B. S., Huang, F. Y., Su, J. Q., Yang, X. R. (2015). pH regulates ammonia-oxidizing
645 bacteria and archaea in paddy soils in Southern China. *Appl Microbiol Biot.* 99:14, 6113-23. doi:
646 10.1007/s00253-015-6488-2

647 Lisa, J.A., Song, B., Tobias, C.R., Hines, D.E. (2015). Genetic and biogeochemical investigation
648 of sedimentary nitrogen cycling communities responding to tidal and seasonal dynamics in Cape
649 Fear River Estuary. *Estuar. Coast. Shelf Sci.* 167, A313-A323. doi: 10.1016/j.ecss.2015.09.008.

650 Liu, S., Shen, L., Lou, L., Tian, G., Zheng, P., Hu, B. (2013). Spatial distribution and factors
651 shaping the niche segregation of ammonia-oxidizing microorganisms in the Qiantang River,
652 China. *Appl. Environ. Microbiol.* 79:13, 4065-4071. doi: 10.1128/AEM.00543-13

653 Marchesi, J.R., Sato, T., Weightman, A.J., Martin, T.A., Fry, J.C., Hiom, S.J., Wade, W.G. (1998).
654 Design and evaluation of useful bacterium-specific PCR primers that amplify genes coding for
655 bacterial 16S rRNA. *Appl. Environ. Microbiol.* 64:2, 795-799. doi: 10.1128/aem.64.2.795-
656 799.199

657 McClain, M.E., Boyer, E.W., Dent, C.L., Gergel, S.E., Grimm, N.B., Groffman, P.M., Hart, S.C.,
658 Harvey, J.W., Johnston, C.A., Mayorga, E., McDowell, W.H., Pinay, G. (2003). Biogeochemical
659 Hot Spots and Hot Moments at the Interface of Terrestrial and Aquatic Ecosystems. *Ecosystems*.
660 6:4, 301-312. doi: 10.1007/s10021-003-0161-9

661 Moin, N.S., Nelson, K.A., Bush, A., Bernhard, A.E. (2009). Distribution and diversity of archaeal
662 and bacterial ammonia oxidizers in salt marsh sediments. *Appl. Environ. Microbiol.* 75, 7461-
663 7468. doi: 10.1128/AEM.01001-09

664 Mosier, A.C., Francis, C.A. (2008). Relative abundance and diversity of ammonia-oxidizing
665 archaea and bacteria in the San Francisco Bay estuary. *Env. Microbiol.* 10, 3002-3016. doi:
666 10.1111/j.1462-2920.2008.01764.x

667 Muyzer, G, De Waal E. C., Uitterlinden A. G. (1993). Profiling of complex microbial populations
668 by denaturing gradient gel electrophoresis analysis of polymerase chain reaction-amplified genes
669 coding for *16S rRNA*. *Appl Env. Microbiol.* 59, 695-700. doi: 10.1128/aem.59.3.695-700.1993

670 Palatinszky, M., Herbold, C., Jehmlich, N., Pogoda, M., Han, P., Von Bergen, M., Lagkouvardos,
671 I., Karst, S.Ø.M., Galushko, A., Koch, H., Berry, D., Daims, H., Wagner, M. (2015). Cyanate as an
672 energy source for nitrifiers. *Nature.* 524:7563, 105-108. doi: 10.1038/nature14856

673 Park, S., Bae, W. (2009). Modeling kinetics of ammonium oxidation and nitrite oxidation under
674 simultaneous inhibition by free ammonia and free nitrous acid. *Process Biochem.* 6, 631-640. doi:
675 10.1016/j.procbio.2009.02.002

676 Rothauwe, J., Witzel, K., Liesack, W. (1997). The Ammonia Monooxygenase Structural Gene
677 *amoA* as a Functional Marker : Molecular Fine-Scale Analysis of Natural Ammonia-Oxidizing
678 Populations. *Appl. Environ. Microbiol.* 63, 4704-4712. doi: 10.1128/aem.63.12.4704-4712.1997

679 Rysgaard, S., Risgaard-Petersen, N., Nielsen, L.P., Revsbech, N.P. (1993). Nitrification and
680 denitrification in lake and estuarine sediments measured by the N dilution technique and isotope
681 pairing. *Appl Environ Microbiol.* 59, 2093-2098. doi: 10.1128/aem.59.7.2093-2098.1993

682 Santoro, A. E., Casciotti, K. L., Francis, C. A. (2010). Activity, abundance and diversity of
683 nitrifying archaea and bacteria in the central California. *Current. Environ. Microbiol.* 12, 1989-
684 2006. doi: 10.1111/j.1462-2920.2010.02205.x

685 Santos, J.P., Mendes, D., Monteiro, M., Ribeiro, H., Baptista, M.S., Borges, M.T., Magalhães, C.
686 (2018). Salinity impact on ammonia oxidizers activity and *amoA* expression in estuarine
687 sediments. *Estuar. Coast. Shelf Sci.* 211, 177-187. doi:10.1016/j.ecss.2017.09.001

688 Schleper, C., Nicol, G.W. (2010). Ammonia-oxidising archaea - physiology, ecology and
689 evolution. *Adv. Microb*, 57, 1-41. doi: 10.1016/B978-0-12-381045-8.00001-1

690 Shen, T., Stieglmeier, M., Dai, J., Urich, T., Schleper, C. (2013). Responses of the terrestrial
691 ammonia-oxidizing archaeon *Ca. Nitrososphaera viennensis* and the ammonia-oxidizing
692 bacterium *Nitrospira multiformis* to nitrification inhibitors. *FEMS Microbiol Letters* 344:2, 121-
693 129. doi:10.1111/1574-6968.12164

694 Smith, C.J., Nedwell, D.B., Dong, L.F., Osborn, A.M. (2006). Evaluation of quantitative
695 polymerase chain reaction-based approaches for determining gene copy and gene transcript

696 numbers in environmental samples. Environ. Microbiol. 8, 804-815. doi:10.1111/j.1462-
697 2920.2005.00963.x

698 Stein, Y., Klotz, G. M. (2016). The nitrogen cycle. Curr. Microbiol. 26, R94-R98. doi:
699 10.1016/j.cub.2015.12.021

700 Stephen, J.R., Chang, Y.J., Macnaughton, S.J., Kowalchuk, G.A., Leung, K.T., Flemming, C.A.,
701 White, D.C. (1999). Effect of toxic metals on indigenous soil beta-subgroup proteobacterium
702 ammonia oxidizer community structure and protection against toxicity by inoculated metal-
703 resistant bacteria. Appl. Environ. Microbiol. 65, 95-101. doi: 10.1128/aem.65.1.95-101.1999

704 Tatti, E., McKew, B.A., Whitby, C., Smith, C.J. (2016). Simultaneous DNA-RNA Extraction from
705 Coastal Sediments and Quantification of 16S rRNA Genes and Transcripts by Real-time PCR. J.
706 Vis. Exp. 112, 54067. doi: 10.3791/54067

707 Taylor, A.E., Zeglin, L.H., Dooley, S., Myrold, D.D., Bottomley, P.J. (2010). Evidence for
708 different contributions of archaea and bacteria to the ammonia-oxidizing potential of diverse
709 Oregon soils. Appl. Environ. Microbiol. 76, 7691-7698. doi: 10.1128/AEM.01324-10

710 Tourna, M., Freitag, T. E., Nicol, G. W., Prosser, J. I. (2008). Growth, activity and temperature
711 responses of ammonia-oxidizing archaea and bacteria in soil microcosms. Env. Microbiol. 10,
712 1357-1364. doi:10.1111/j.1462-2920.2007.01563.x

713 Vajrala, N., Bottomley, P.J., Stahl, D.A., Arp, D.J., Sayavedra-Soto, L.A. (2014). Cycloheximide
714 prevents the *de novo* polypeptide synthesis required to recover from acetylene inhibition in
715 *Nitropumilus maritimus*. FEMS Microbiol. Ecol. 88, 495-502. doi: 10.1111/1574-6941.12316

716 van Kessel, M.A., Speth, D.R., Albertsen, M., Nielsen, P.H., Op den Camp, H.J., Kartal, B., Jetten,
717 M.S., Lücker, S. (2015). Complete nitrification by a single microorganism. *Nature*. 528, 555-559.
718 doi: 10.1038/nature16459

719 Walkup, J., Freedman, Z., Kotcon, J., Morrissey, E.M. (2020). Pasture in crop rotations influences
720 microbial biodiversity and function reducing the potential for nitrogen loss from compost. *Agr.*
721 *Ecosyst. Environ.* 304, art. no. 107122. doi: 10.1016/j.agee.2020.107122

722 Wang, J., He, Y., Zhu, J., Guan, H., Huang, M. (2017). Screening and optimizing of inhibitors for
723 ammonia-oxidizing bacteria in sediments of malodorous river. *App. Microbiol. Biotechnol.*
724 101:15, 6193-6203. doi:10.1007/s00253-017-8318-1.

725 Wright, C.L., Schatteman, A., Crombie, A.T., Murrell, J.C., Lehtovirta-Morley, L.E. (2020).
726 Inhibition of ammonia monooxygenase from ammonia-oxidizing archaea by linear and aromatic
727 alkynes. *Appl. Environ. Microbiol.* 86:9, art. no. e02388. doi:10.1128/AEM.02388-19. Wuchter,
728 C., Abbas, B., Coolen, M.J.L., Herfort, L., van Bleijswijk, J., Timmers, P., Strous, M., Teira, E.,
729 Herndl, G.J., Middelburg, J.J., Schouten, S., Damsté, J.S.S. (2006). Archaeal nitrification in the
730 ocean. *Proc. Natl. Acad. Sci.* 103: 12317-12322. doi: 10.1073/pnas.0600756103

731 Xu, S., Zhang, Z., Jia, G., Yu, K., Lei, F., Zhu, X. (2020). Controlling factors and environmental
732 significance of BIT and $\delta^{13}\text{C}$ of sedimentary GDGTs from the Pearl River Estuary, China over
733 recent decades. *Estuar. Coast. Shelf Sci.* 233, art. no. 106534. doi: 10.1016/j.ecss.2019.106534

734 Yang, W. H., Ryals, R. A., Cusack, D. F., Silver, W. L. (2017). Cross-biom assessment of gross
735 soil nitrogen cycling in California ecosystems. *Soil Biol. Biochem.* 107, 144-155.
736 doi:10.1016/j.soilbio.2017.01.004

737 Zhang, L.M., Duff, A.M., Smith, C.J. (2018). Community and functional shifts in ammonia
738 oxidizers across terrestrial and marine (soil/sediment) boundaries in two coastal Bay ecosystems.
739 *Env. Microbiol.* 20:8, 2834-2853. doi:10.1111/1462-2920.14238

740 Zhu, G., Wang, S., Wang, W., Wang, Y., Zhou, L., Jiang, B., Op Den Camp, H.J.M., Risgaard-
741 Petersen, N., Schwark, L., Peng, Y., Hefting, M.M., Jetten, M.S.M., Yin, C. (2013). Hotspots of
742 anaerobic ammonium oxidation at land-freshwater interfaces. *Nat. Geosci.* 6:2, 103-107. doi:
743 10.1038/ngeo1683